Structural Integrity Evaluation of the Wing Structure at High Stress Concentration Regions

Anish Nair [1] K.M Narkar [2]
[2]Professor
[1,2]Department of Mechanical Engineering
[1,2]University of Pune

Abstract— Structural integrity is an important factor to be considered when it comes to the safety of aircrafts. Structural integrity is the ability of a structure to withstand a designed service load resisting structural failure due to fracture, deformation and fatigue. In this current work, stress analysis of a wing box with a cutout in the bottom skin for fuel access is carried out to find the critical region where there is a possibility of fatigue crack initiation. Crack arrest capability of the bottom skin is determined by the damage tolerance analysis. Static testing of the scaled down model of the bottom skin is carried out using the universal testing machine.

Key words: Wing Structure, Tolerance Analysis, Cutouts, Stiffened Panels, Integral Technique

I. INTRODUCTION

The main lift generating components in the aircraft structure is the wings. About 80% of the lift load is taken by the wings. Another function of the wing is that they are also used as fuel tanks in commercial aircrafts. As functional requirement point of view cutouts are provided in the bottom skin of the wing. During flight, the bottom skin of the wing is in the tension stress field whereas the top skin in the compression stress field. Due to this, the cutouts and the rivet holes on the bottom skin act as stress raisers and are the probable locations of fatigue crack initiation. If such a crack initiates it is necessary to arrest that crack. This is done by the damage tolerance analysis. Damage tolerance is the property of a structure relating to its ability to sustain defects safely until repair can be affected.

II. LITERATURE SURVEY

This paper considers most common problems related with structural integrity of civil aircraft in Russia taking into account the development of regulatory requirements, prevention of multiple site fatigue damages, improvements of crack resistance of structural materials, optimizations of aircraft type structures, development of methods for residual strength analyses of stiffened structures as well as for crack growth rates under random service loading spectra, experimental results for crack resistance degradation, methods to prevent structural failure for long operated aircraft due to corrosion.[1]

This paper the author presents the methodologies for damage tolerant evaluation of stiffened panels under fatigue loading. The two major objectives of damage tolerant evaluation, namely, the remaining life prediction and residual strength evaluation of stiffened panels have been discussed. Eccentric and concentric stiffeners have been considered. Stress intensity factor (SIF) for a stiffened panel has been computed by using parametric equations of numerically integrated modified virtual crack closure integral technique. Various methodologies for residual strength evaluation, namely, plastic collapse condition, fracture toughness criterion and remaining life approach have been explained. Effect of various stiffener type and stiffener sizes on residual strength and remaining life has been studied under constant amplitude load. From the studies, it has been observed that the predicted life is significantly higher with eccentric and concentric stiffener cases compared to the respective unstiffened cases. The percentage increase in life is relatively less in the case of eccentric stiffener compared to that of concentric stiffener case for the same stiffener size and moment of inertia. From the studies, it has also been observed that the predicted residual strength using remaining life approach is lower compared to other methods, namely, plastic collapse condition and fracture toughness criterion and hence remaining life approach will govern the design. It is noted that residual strength increases with the increase of stiffener size.[2]

This paper the fatigue life of critical structural locations in the wing of the Finnish Air Force (FAF) Hawk jet trainer was estimated. This was done by using calibration coefficients determined by means of a virtual fatigue test. The load distribution and load history of the manufacturer's Full Scale Fatigue Test (FSFT) was first reproduced by using an FE model. The peaks through histories of the stresses in the critical structural locations were determined. The calculated histories were then used as an input in the virtual fatigue test calculations. A fatigue life calibration coefficient based on the ratio of virtual fatigue test estimates versus FSFT results was calculated. It was determined separately to each selected critical location. On the basis of flight measurement data, aerodynamic loads calculation and FE models were calibrated and the stress histories of critical items in average usage by the FAF were determined. By correcting the results of the fatigue life analyses using the calibration coefficients produced by the virtual fatigue test, more accurate fatigue life estimates in FAF usage could be made. The calibration of results against in reality detected structural damages improves the accuracy of analytical methods allowing the correction of differences between the actual structure and the idealized FE model. Since new fatigue tests are not required, it is possible to make reasonable fatigue life estimates at lower costs compared with traditional methods that require fatigue tests.[3]

This paper author presents the state of the art about fatigue of structure sand materials. Aircraft accidents and incidents were milestones. New concepts were proposed related to structural design, material selection, production techniques, inspection procedures and load spectra. Extensive research efforts have been spent. Our understanding of fatigue damage problems increased significantly. Simultaneously our tools to tackle problems have been developed to a high potential efficiency. And still,

there are problems. The present paper is a personal impression of evaluating experience, design aspects, predictions and experiments associated with damage tolerance of aircraft structures. [4]

III. GEOMETRIC MODELING OF THE WING BOX

Material used for the analysis of Wing panel is Aluminum 2024-T351 (Al 2024-T351). Wing box is created using the CATIA software tool and then it was imported to FE tool. The assembled view of the Wing box containing bottom skin, spars, top skin and rib is shown in the figure below.

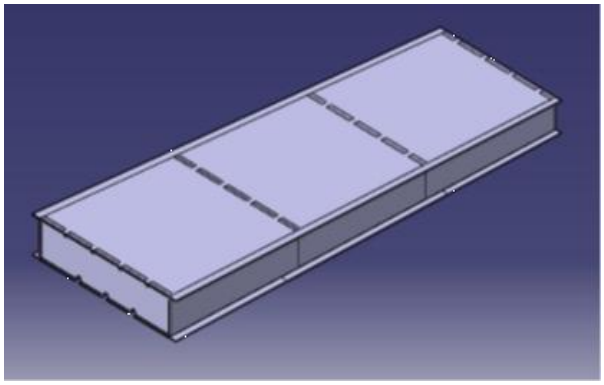

Fig. 1: Wing Box

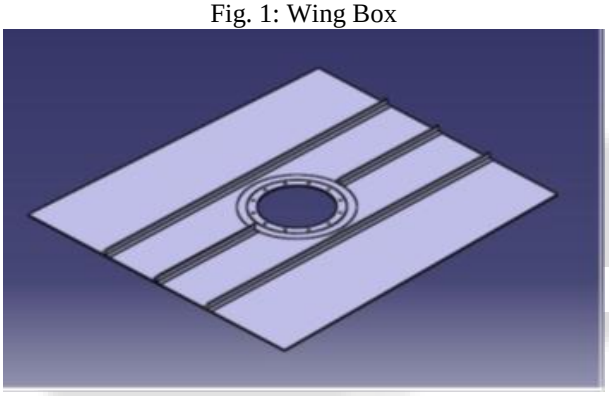

Fig. 2: Bottom Skin of Wing Box

IV. STRESS ANALYSIS OF THE WING BOX

The finite element model of the wing box is shown in the figure below. First we carry out the global analysis. In global analysis the rivet holes are not considered The bending moment acting at the end of the wing box is calculated by the lift equation and is found to be 4640.16 kg. The boundary conditions are applied to the finite element model and the stress analysis is carried out.

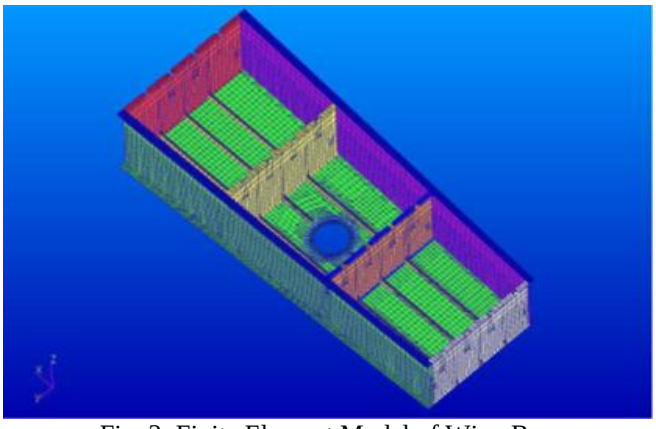

Fig. 3: Finite Element Model of Wing Box

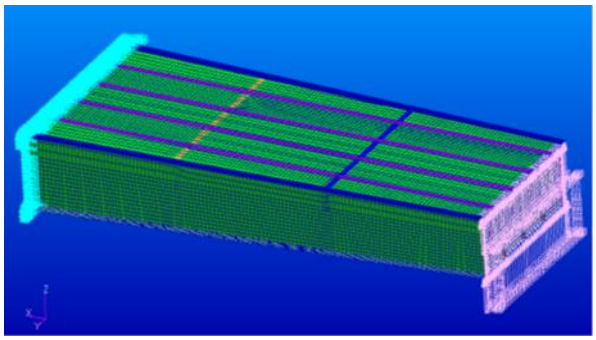

Fig. 4: Boundary Conditions Applied

The maximum stress is found at the edge of the cutout. due to the eccentricity in loading because of the thickness variation near the cutout we get two values of stress Z1 and Z2. Maximum stress at Z1 is 19.5 kg/mm2 and maximum stress at Z2 is 16.4kg/mm2. The total maximum stress is obtained by taking the average of the two which is 18 kg/mm2.

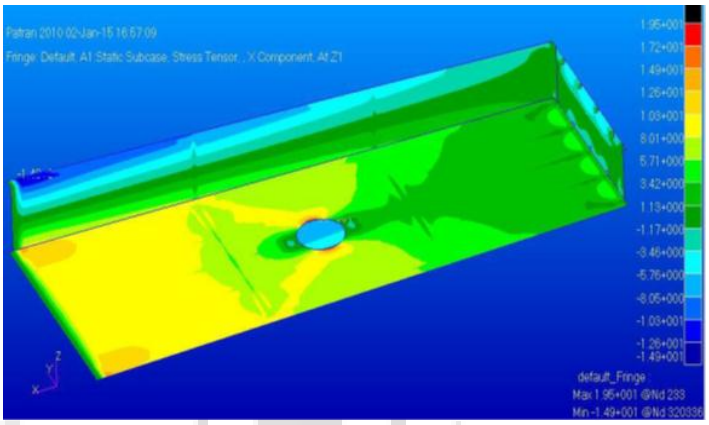

Fig. 5a: Stress Contour (Z1)

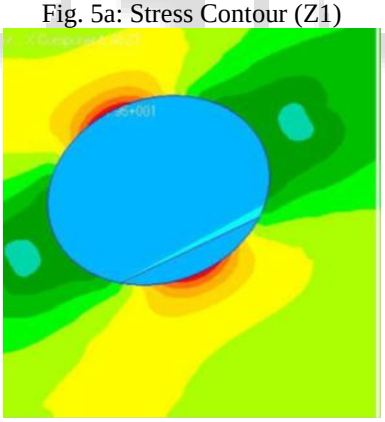

Fig. 5b: Close Up View

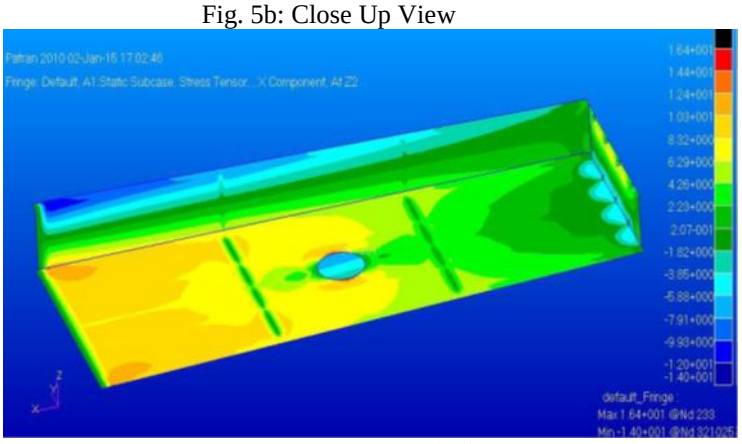

Fig. 6a: Stress Contour (Z2)

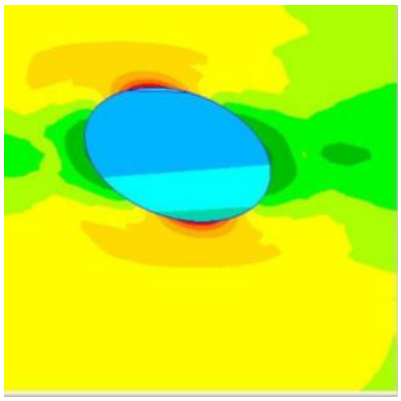

Fig. 6b: Close Up View

Following the global analysis, local analysis is carried out considering the critical region from the global analysis and also considering the rivet holes. The finite element model of the local model is shown in the figure below

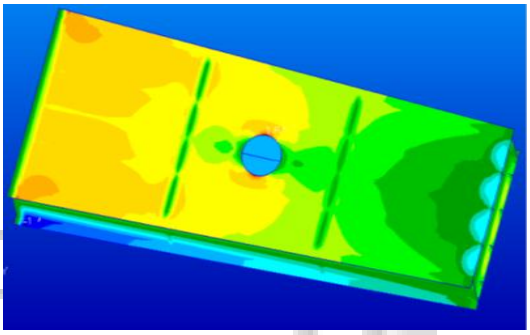

Fig. 7: Panel to Be Considered For Local Analysis

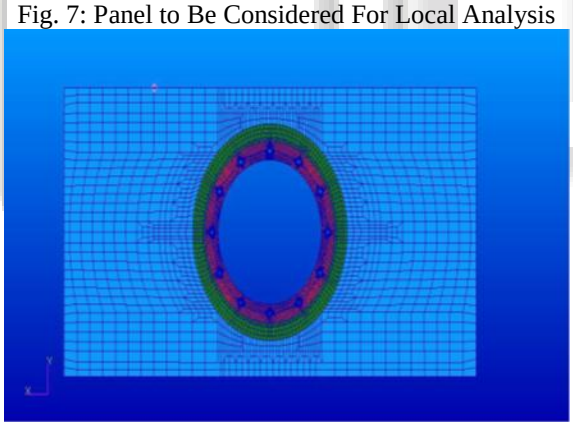

Fig. 8: Finite Element Model of Local Model

The maximum stress from the local analysis is found to be 39 kg/mm2 which is the nodal value near the rivet holes. A stress distribution graph is plotted to get the elemental stress value as shown in the fig. from the graph, we get the stress value as 33kg/mm2

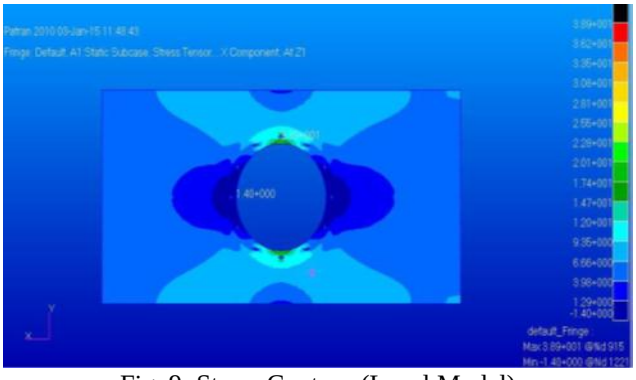

Fig. 9: Stress Contour (Local Model)

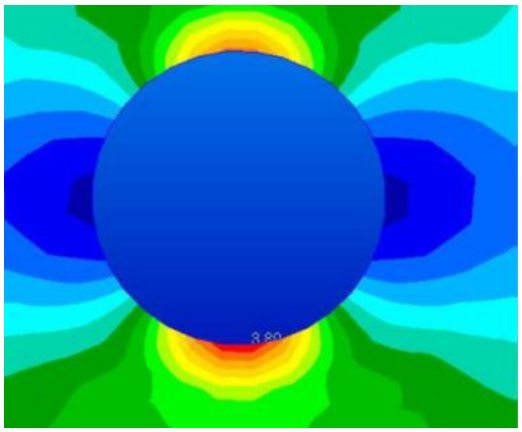

Fig. 10: Close Up View

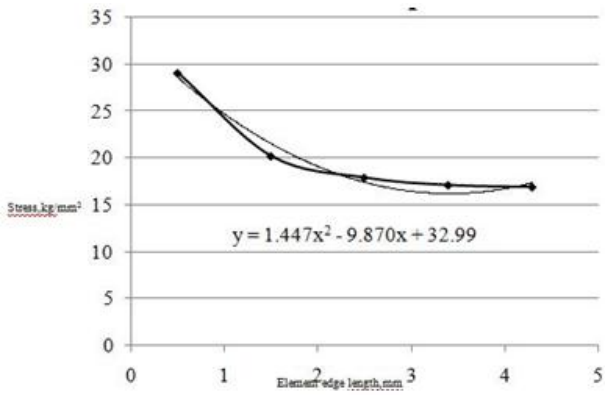

Fig. 11: Stress Distribution

V. DAMAGE TOLERANCE ANALYSIS

Due to the repeated fatigue loading, there is a possibility of fatigue crack initiation at the critical locations. These critical locations are found out from the local and global analysis. Now we will simulate a small crack in the local model of various lengths and we will find out the stress intensity factors for the different crack lengths. The stress intensity factor is found out by the Modified Virtual Crack Closure Integral (MVCCI) method. It is given by

$$K_I = \sqrt{(G \times E)} \quad (5.1)$$

Where, G = Strain energy release rate, N/mm

E = Young's Modulus, N/mm^2

The strain energy release rate, G is given by

$$G = 1/(2 \times \Delta a) \times \Delta v \times (F/t) \quad (5.2)$$

Where, Δa = element edge length near the crack tip, mm

Δv = relative displacement of the nodes near the crack tip, mm

F = Force at the crack tip, N

T = thickness of the skin, mm

The values of Δa, Δv, F and t are obtained from the finite element analysis results. For a crack length of 2mm we get the following values

$\Delta a = 1$ mm

$\Delta v = 0.0153$ mm

F = 121.86 N

t = 5 mm

By substituting these values in equation (ii), we get value of G as 0.1864. now substituting the value G and Young's modulus in equation (i), we get $K_I = 11.21$ Mpa$\sqrt{m}$

which is the stress intensity factor for a crack length of 2mm. similarly the SIF values for different crack lengths are calculated. These are shown in the table below

Crack length '*a*' mm	Thickness '*t*' mm	Element edge length 'Δa' mm	Relative displacement 'ΔV' mm	Grid point force '*F*' N	Strain energy release rate '*G*'	Stress intensity factor 'K_I' MPa$\sqrt{m}$
2	5	1	0.0153	121.86	0.1864	11.21
4	5	1	0.0176	141.09	0.2483	12.93
6	5	1	0.0209	165.51	0.3459	15.26
8	5	1	0.0253	197.99	0.5003	18.36
10	5	1	0.0378	269.48	1.0186	26.19
14	4	1	0.0401	248.37	1.2449	28.95
18	4	1	0.0406	251.17	1.2747	29.30
22	4	1	0.0413	254.93	1.3161	29.77
26	4	1	0.0420	259.33	1.3165	30.28
30	4	1	0.0429	264.76	1.4198	30.92
34	4	1	0.0445	274.25	1.5255	32.06
38	3	1	0.0482	223.87	1.7984	34.81
42	3	1	0.0464	215.64	1.6676	33.52
46	3	1	0.0249	116.54	0.4836	18.05
50	3	1	0.0224	125.24	0.4876	17.74

Table 1: stress intensity factor

A graph of SIF vs crack length is plotted and is shown below. From the graph we can observe that as the crack length increases, the SIF value also increases. But this trend changes when the crack approaches stringer location. Near the stringer location the SIF value decreases which gives us an indication of crack arrest capability of the stringer.

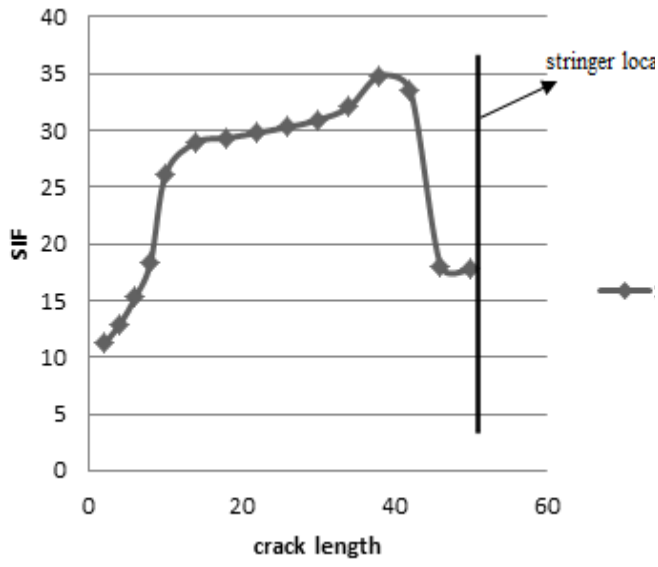

Fig. 12: SIF vs Crack length

Similarly the residual length for the various crack lengths are calculated by the formula

Residual strength = $(K_{IC} / K_I) \times \sigma_{remotely\ applied}$ (5.3)

Where, K_{IC} = fracture toughness

K_I = stress intensity factor

σ = remotely applied stress

The residual strength values are tabulated below kg/mm2

Table. 2: Residual Strength

Crack length, mm	Residual strength, kg/mm^2
2	35.53
4	30.81
6	26.10
8	21.69
10	15.20
14	14.09
18	13.93
22	13.71
26	13.47
30	13.19
34	12.72
38	12
42	12.46
46	23.14
50	23.55

A graph of Residual strength vs. crack length is plotted. From the graph we can observe that as the crack length increases the residual strength of the bottom skin goes on decreasing. But as the crack length approaches the stringer location, there is an increase in the value of residual strength which shows the crack arresting capability of the stringer.

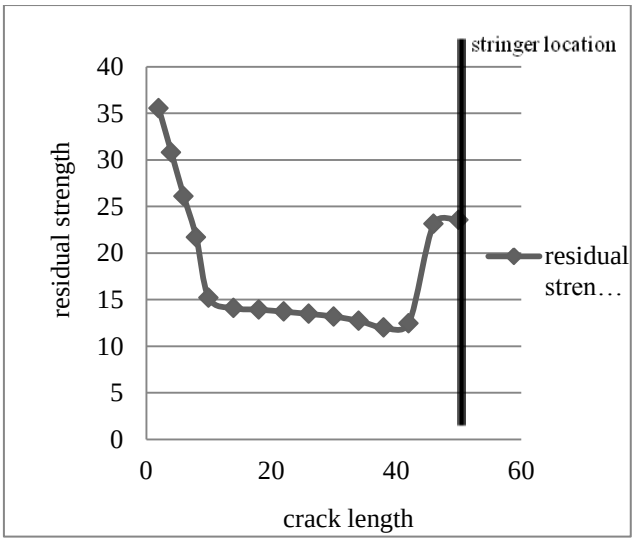

Fig. 13: Residual Strength Vs. Crack Length

VI. EXPERIMENTAL TESTING OF THE BOTTOM SKIN PANEL

A scaled down model of the local panel is fabricated for the experimental testing. Strain gauges are mounted at the critical locations to capture the value of strain. The model is tested on the universal testing machine

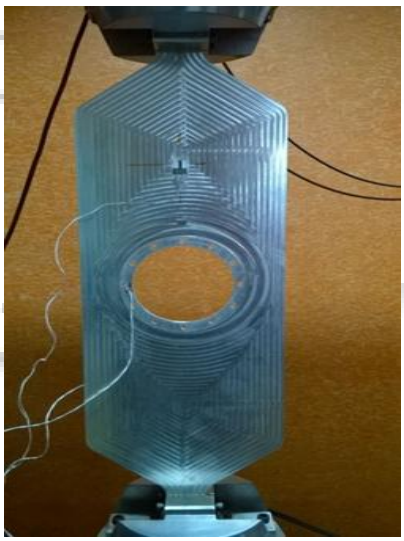
Fig. 14: Test Specimen

Following results are obtained from the testing

Load(kg)	Strain gage 1 (μ strain)	Strain gage 2 (μ strain)
100	65	133
200	132	268
300	201	399
400	273	531
500	345	659

Table 3: Strain Gage Readings

From the stress analysis of the local model, we get the maximum stress as 33 kg/mm2

$$\sigma_{local} = 33 kg/mm^2$$

The net cross sectional area of the panel is 352 mm^2.

Therefore, $\sigma_{nominal} = 3318/352$

$= 9.42 \ kg/mm^2$

Stress concentration factor, $Kt = \sigma_{local} / \sigma_{nominal}$

$= 33 / 9.42$

$=3.50$

From the experimental testing, we get the following strain values

Gauge 1 = 345 μ strain

Gauge 2 = 659 μ strain

Gauge 3 = 189 μ strain

Here we will take the average of gauge 1 and gauge 2. The reason for this is because of the thickness variation built on one side, eccentricity will be created in loading. Due to this the panel experiences out of plane displacement. Therefore we can observe the variation in the strain values.

$\varepsilon_{local} = (345+669) / 2$

$= 502\mu$ strain

$\varepsilon_{nominal} = 189\mu$ strain

Stress concentration factor, $Kt = \varepsilon_{local} / \varepsilon_{nominal}$

$=502 / 189$

$= 2.65$

The small variation in the analysis and experimental value is because in the analysis the values are obtained at the edge of the rivet holes. But practically it is very difficult to mount the strain gauges at the end of the rivet hole, hence it is mounted some distance away from the edge of the rivet hole. Hence there is a small variation in the stress concentration values.

VII. CONCLUSION

Structural integrity evaluation was carried out by considering a wing box with a fuel access cutout. Finite element analysis was used for the stress analysis of the structure. Local analysis was carried out by considering a panel with cutout and small rivet holes. The maximum tensile stress was identified at one of the rivet holes and it is found to be 33 kg/mm2. A panel was fabricated with scaled down dimensions using CNC machining. Test specimen was prepared by putting strain gages near the predicted high stress locations. Static testing was carried out using the universal testing machine. Stress was calculated using the experimentally measured strain values and compared with the analytically obtained values. Experimental results correlate well with the analysis results. Stress intensity factor (SIF) calculations were carried out for the crack originating from the rivet hole using MVCCI method. Variation of SIF as a function of crack length is plotted. SIF increases with the increase in crack length, but shows decreasing trend near the stiffener location.

REFERENCES

[1]. Nesterenko G.I, Nesterenko B.G, "Ensuring Structural Damage Tolerance of Russian Aircraft", International Journal of Fatigue 31, pp 1054–1061, 2009

[2]. Rama Chandra Murthy A, PalaniG.S, IyerNagesh R, "Damage tolerant evaluation of cracked stiffened panels under fatigue loading", Sadhana, Vol. 37, Part 1, pp. 171–186, 2012

[3]. Tikka Jarkko, Patria, "Fatigue life evaluation of critical locations in aircraft structures using virtual fatigue test", ICAS 17, pp 208-221, 2002

[4]. SchijveJaap, "Fatigue damage in aircraft structures, not wanted, but tolerated?", International Journal of Fatigue 31, pp 998–1011, 2009

